Positron annihilation in syndiotactic polystyrene containing α and β crystalline forms

B.G. Olson[a], T. Prodpran[b], A.M. Jamieson[b], S. Nazarenko[b,*]

[a]*Department of Physics, Case Western Reserve University, Cleveland, OH 44106, USA*
[b]*Department of Macromolecular Science, Center for Applied Polymer Research, Case Western Reserve University, Cleveland, OH 44106, USA*

Abstract

Positron annihilation lifetime spectroscopy (PALS) measurements were performed on a series of syndiotactic polystyrene (s-PS) samples crystallized from the melt state. These s-PS samples contained either pure α or β forms with various crystallinities. The α and β crystalline forms are known to have densities very similar to the amorphous phase. The low-density is believed to be associated with nanovoids or nanochannels, existing between the polymer chains in crystalline s-PS. A question can be raised whether positronium can form and annihilate in these low-density crystalline structures. In analyzing the PALS spectra, it was found that four distinct lifetime components gave the best fit for all studied samples. The longest lifetime component ($\tau_4 = 2–3$ ns) exhibits thermal expansion behavior typical of amorphous polymers, while the second longest lifetime ($\tau_3 \sim 0.8$ ns) is constant, independent of temperature, crystallinity and tacticity. For all semicrystalline and amorphous s-PS samples, the PALS spectra were found to be essentially indistinguishable, with remarkably similar lifetimes and intensities. This behavior implies that *ortho*-positronium can indeed form in the low-density crystal structures of s-PS. Two possibilities for *ortho*-positronium annihilation in the semicrystalline polymer were proposed and analyzed: (a) *ortho*-positronium annihilates in the crystal phase with a lifetime characteristic of the nanochannel dimensions; (b) *ortho*-positronium rapidly diffuses into the amorphous phase and annihilates with a lifetime typical of that phase. No evidence for the existence of a lifetime component characteristic of the crystal nanochannels was found, indicating that the second annihilation mechanism is dominant. © 2002 Elsevier Science Ltd. All rights reserved.

Keywords: Syndiotactic polystyrene; Crystalline structure; Positron annihilation

1. Introduction

Syndiotactic polystyrene shows a complex polymorphic behavior. The various crystalline forms differ in the conformational order, and in the mode of crystalline packing of chains having the same conformational order. Two lyotropic crystalline forms, gamma and delta, contain helical chains, whereas two thermotropic forms, α and β, exhibit planar zigzag conformation order [1]. The structure of the β form, Fig. 1a, is characterized by an ordinary orthorhombic chain packing. The calculated crystalline density of the β form is 1.068 g/cm³ [2,3]. While this density is larger than that of amorphous s-PS (1.046 g/cm³), it represents only a 1.7% increase, indicating fairly loose crystal packing, compared to other semicrystalline polymers, which typically have a crystalline density 10–15% larger than the amorphous phase [4].

The α form of s-PS is unusual and its precise structure remains an open question. Two possible models of chain packing in the α crystalline phase are shown in Fig. 1b and c, proposed by Greis et al. [5] and De Rosa et al. [6,7], respectively. It is well accepted that in the α form, chains are packed in relatively dense groups of three (triplets) with the backbones at the core and phenyl rings pointed towards the periphery. The bulky nature of the triplets makes efficient packing difficult, giving rise to a relatively loose superstructure. The overall crystalline density of the α form is 1.033 g/cm³ [5], which is not only smaller than that of the β phase, but also smaller than the amorphous phase density, by 1.6%. This behavior is unusual among synthetic polymers and has previously only been reported for one other material, poly(4-methyl-1-pentene) [8], which exhibits a comparable density difference between crystalline and amorphous phases.

Despite a significant difference in the specific arrangement of the triplets in the α forms proposed by Greis and

* Corresponding author.
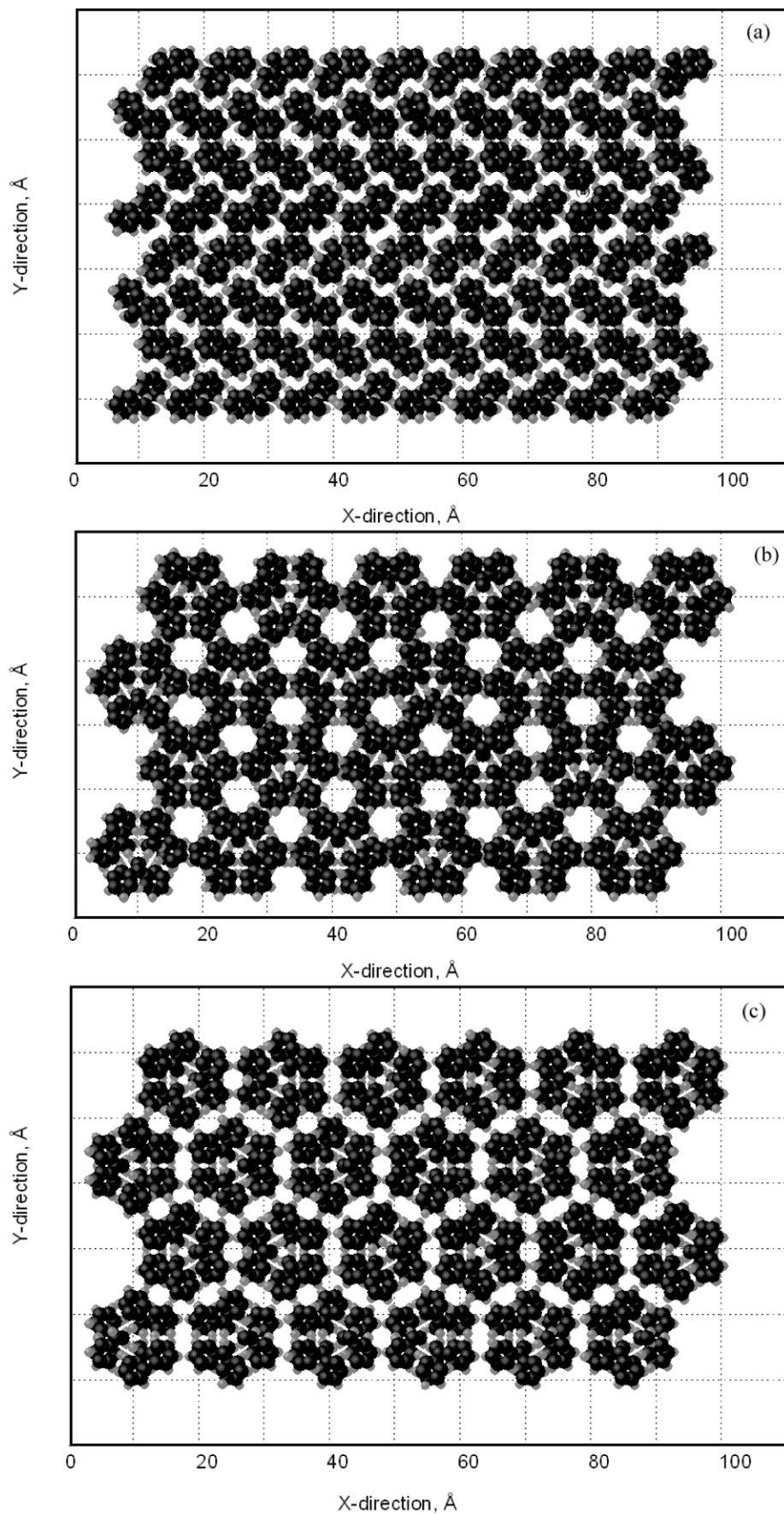 *E-mail address:* sin@po.cwru.edu (S. Nazarenko).

Fig. 1. Scale models of β and α crystalline forms of s-PS: (a) β-crystalline form; (b) α-crystalline form (Greis); (c) α-crystalline form (De Rosa).

De Rosa, both models predict the same overall density. However, each crystal structure exhibits a different distribution of unoccupied space. In the Gries model, the structure exhibits relatively large open channels surrounding the triplets, each having an almost circular aperture of about 5 Å in diameter. In the De Rosa model, the unoccupied space almost uniformly surrounds each triplet in the form of hollow hexagonal channels with an aperture of about 3–4 Å. Thus each structure predicts the presence of nanochannels in the α phase. The question whether the β form also contains channels in the crystal structure remains open. Noting that the density of the β crystal form is only slightly larger than the density of the amorphous phase, the possibility that comparable nanovoids exist between the chains in these crystalline forms cannot be ruled out. Finally, we point out that, since the chain orientation is perpendicular to the lamellar fold surface, the channel lengths in these crystals must be comparable to the lamellar thickness of about 100 Å for semicrystalline s-PS [5].

Experimental evidence for the existence of nanochannels in s-PS crystals is scant. One piece of evidence is the existence of increased permeability to small gas molecules of s-PS containing the α crystal form [9,10]. These studies show that permeability to O_2 and CO_2 increases with the degree of crystallinity when the α form is present, but not when the β form is present. The analysis suggests that the effect is due to enhanced diffusion of the gas molecules rather than enhanced solubility. The proposed nanochannels in the α form are large enough to accommodate the O_2 and CO_2 molecules, whereas those in the β form may be too small.

Positron annihilation lifetime spectroscopy (PALS) is commonly used to probe the free volume properties of amorphous polymers [11–15]. In polymers, one mechanism of positron annihilation involves formation of *ortho*-positronium, a short-lived complex with an electron, in the free volume void spaces. Thus, the relative amount of *ortho*-positronium that forms (proportional to the intensity of the *ortho*-positronium annihilation component in the PAL spectrum), can be related to the numbers of voids. It has also been established that the *ortho*-positronium lifetime in a polymer gives a measure of the average free volume void size. PALS has also been employed to study the structure of various semicrystalline polymers [16–23]. In most cases, the *ortho*-positronium annihilation intensity is reported to decrease with increase in crystallinity, suggesting that *ortho*-positronium cannot form in the ordered phase due to the high density. As a result, the *ortho*-positronium lifetime probes free volume hole sizes related solely to the amorphous phase.

The question arises, however, whether *ortho*-positronium can form in the low-density, porous, crystalline structure of s-PS. Semicrystalline syndiotactic polystyrene containing the α crystal form has previously been studied at room temperature via PALS [24]. The *ortho*-positronium lifetime was observed to be very similar to that of

amorphous atactic polystyrene (a-PS). The *ortho*-positronium intensity, however, showed a significantly lower value for semicrystalline s-PS (22%) as compared to a-PS (30%). It was, therefore, concluded that *ortho*-positronium does not form in the α crystal structure of s-PS, and forms only in the amorphous phase. The goal of this work is to investigate more thoroughly this behavior by comparing the PALS spectra of s-PS containing varying amounts of either pure α or pure β crystal forms, with that of amorphous s-PS and a-PS.

2. Experimental

2.1. Materials

Syndiotactic polystyrene with average molecular weight $M_W \cong 300,000$ g/mol and polydispersity $M_W/M_N \cong 2$ was supplied by the Dow Chemical Company, Midland, MI, in pellet form. Atactic polystyrene, with a molecular weight and polydispersity similar to that of the syndiotactic form, was also supplied by the Dow Chemical Company.

2.2. Preparation of amorphous syndiotactic and atactic polystyrene

Amorphous samples in the form of 40 μm thin sheets were prepared by compression molding of melted pellets between two polished steel platens. The pellets were placed in a press preheated to 315 °C for 45 min without pressure. The pressure was subsequently increased to 30,000 psi and released; this cycle was repeated two times to insure that the plaques are free of bubbles. Finally, the platens were held at 30,000 psi for 5 min and then released. The samples were then rapidly quenched into an ice–water mixture and then dried under vacuum.

2.3. Preparation of semicrystalline s-PS containing α crystalline form

Samples containing pure α form with various degrees of crystallinity were prepared using isothermal crystallization from the melt. Initially, the sample was degassed as above, but with the press preheated to 280 °C, and then the sample with platens was quickly transferred to a convection oven preset at the crystallization temperature of $T_c = 260$ °C. In the oven the samples were isothermally crystallized for different times to obtain various degrees of crystallinity. Finally, after the crystallization was complete, the samples were rapidly quenched in the ice–water mixture and then dried under vacuum.

2.4. Preparation of semicrystalline s-PS containing β crystalline form

Samples containing the β crystal form, with various

degrees of crystallinity, were prepared by a method similar to that of the α form, but with the press preheated to 350 °C, a preheating time of 10 min, and the isothermal crystallization was performed at 250 °C.

2.5. Measurements

The crystalline structure was studied using wide-angle X-ray scattering measurements conducted with Phillips Model APD 3520 automatic powder diffractometer using nickel filtered Cu Kα radiation (wavelength, 1.542 Å). Powder samples were scanned within scattering angle range 2θ from 5 to 30° at 0.001°/min.

Density was measured using a gradient column constructed from a solution of diethylene glycol/isopropanol in accordance with ASTM-D 1505 Method B. The column was calibrated with glass floats of known density. Small pieces (~ 25 mm^2) were placed in the column and allowed to equilibrate before the measurements were taken. The experimental error of the density measurements did not exceed ± 0.0005 g/cm^3. The crystalline volume fraction was calculated from density using a simple two-phase model assuming constant density of amorphous and crystalline phases $\phi_c = (\rho - \rho_a)/(\rho_c - \rho_a)$, where ρ, ρ_c, and ρ_a, are the densities of the sample, pure crystalline and pure amorphous phases.

Positron annihilation lifetime measurements were taken by a fast–fast coincidence system [25] which has a time resolution function composed of a sum of two gaussians with relative intensities 90.2 and 9.8%, and full width at half maximum (FWHM) of about 230 and 330 ps, respectively, with the exact value for FWHM determined for each spectra. The relative intensities were determined by analyzing spectra obtained from a [207]Bi radioactive source, which emits a 1.06 MeV γ-ray followed shortly by a 0.570 MeV γ-ray, with an equivalent lifetime of 188 ps. All spectra were analyzed with the fitting software package PATFIT [26]. The positron emitter was [22]Na, which emits a e^+ followed by a 1.28 MeV γ-ray a few picoseconds later. The lifetime of the positron was measured by the time between the 1.28 MeV 'birth' γ-ray and one of the 0.511 MeV 'death' γ-rays from the positron annihilating with an electron in the sample. The radioactive sodium isotope was obtained in salt form as [22]NaCl, of which 20 μCi was placed in a sealed pouch of aluminum foil, which was then sandwiched between two identical pieces of polymer, each at least 1 mm thick, to be measured. All lifetime spectra were binned into 4096 channels, with a channel width of 10.7 ps, and collected for 90 min to get at least 1.5×10^6 counts. Each sample was measured at room temperature with data collection starting immediately after source insertion. This procedure was strictly adhered to in order to minimize radiation effects [27–29], and to make sure each sample had the same radiation exposure history. Temperature scans were performed by lowering the temperature to -100 °C over a period of 2 h, then
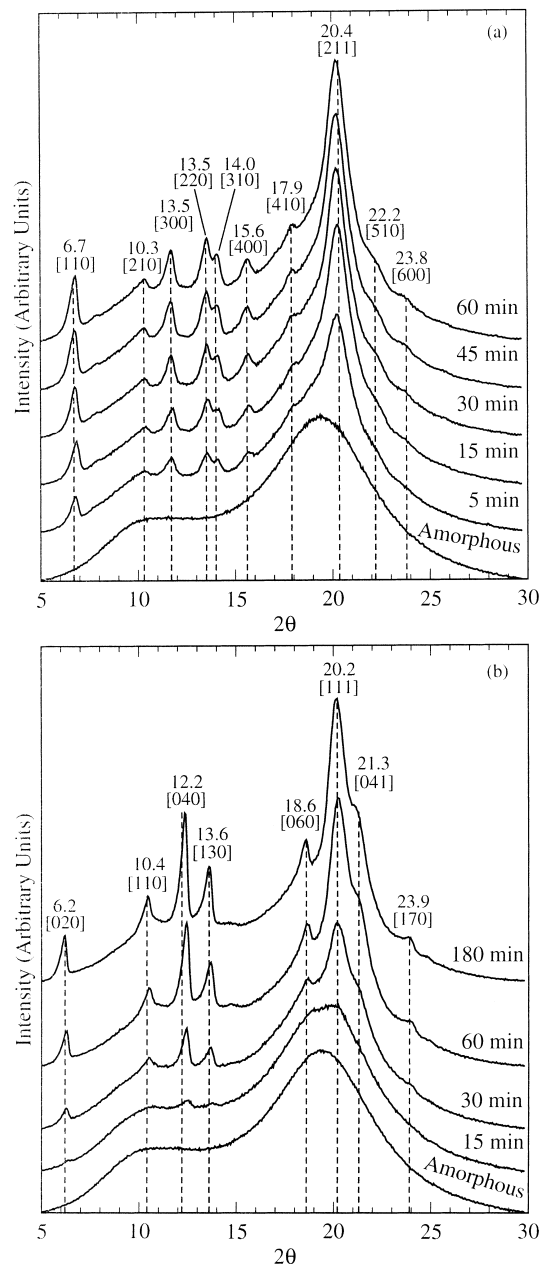

Fig. 2. WAXS diffractograms of amorphous and semicrystalline s-PS: (a) molded at 280 °C and isothermally melt-crystallized at 260 °C for various times; (b) molded at 330 °C and isothermally crystallized at 250 °C for various times.

sequentially increasing the temperature by 10 °C intervals, collecting a spectrum at each step.

3. Results and discussion

3.1. Characterization of crystalline structure

The crystallographic structure of α and β crystal forms of s-PS has been intensively studied for the last 10 years primarily using WAXS [1–3,6,7,30,31]. The proposed
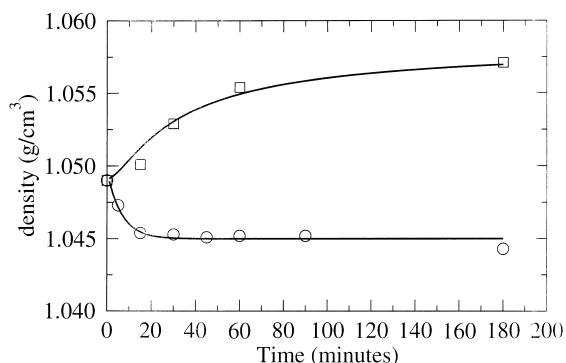
Fig. 3. Dependence of density on crystallization time for melt-crystallized s-PS following procedures for α (○) and β (□) forms.

crystallographic models are described in Section 1. This section aims primarily to present the WAXS data confirming that the crystallization conditions utilized in this work indeed resulted in the formation of pure α and β crystalline forms based on the known WAXS peak assignments.

Fig. 2a shows WAXS diffractograms of samples compression molded at 280 °C and melt crystallized at 260 °C for various times. The corresponding maxima are located at $2\theta = 6.7(110)$, 10.3 (210), 11.7 (300), 13.5 (220), 14.0 (310), 15.6 (400), 17.9 (410), 20.4 (211), 22.2 (510) and 23.8° (600). Maxima at $2\theta = 6.7$, 11.7, 13.5, 17.9, 20.4, 22.2 and 23.8° are generally characteristic of the α crystal form of s-PS [5–7]. Three additional peaks in the diffractograms in Fig. 2a, at $2\theta = 10.3$, 14 and 15.6°, are specific for the limiting ordered modification, α″, of the α form [6,7]. These three peaks are absent in the case of the limiting disordered modification, α′, obtained upon cold crystallization. Fig. 2b shows WAXS diffractograms of

samples compression molded at 330 °C and melt crystallized for various times at 250 °C. All samples reveal the diffraction pattern characteristic of the pure β crystalline form. Specifically, the peaks at $2\theta = 6.2(020)$, 10.4 (110), 12.2 (040), 13.6 (130), 18.6 (060), 20.2(111), 21.3 (041), 23.9 (170) and 24.9° (080), are all attributed to the β form [1,3,6,7,31].

The intensity of the WAXS peaks characteristic of the α and β forms, in Fig. 2a and b, increases with increasing isothermal crystallization time, indicative of the increase in crystallinity. Fig. 3 shows the corresponding dependence of the density for melt-crystallized s-PS versus isothermal crystallization time. As expected the density decreases initially, and then levels off at longer times, when the low-density α crystal structure is formed, and increases initially and levels off at long times when the more dense β crystal structure is formed.

Several s-PS samples containing the α and β crystalline phase, as well as amorphous s-PS and a-PS were chosen for PALS measurements. These samples are listed in Table 1 together with the measured densities and the crystallinities as determined from the density.

3.2. PALS measurements

The PALS spectra for all samples were analyzed with PATFIT [26] for three- and four-components. For all samples a four-component fit was slightly better with variances all below a value of 1.1. A three-component fit had variances in the range of 1.08–1.3. To further verify the validity of using a four-component fit, several spectra were obtained with a total of 5 million counts for better statistics.

Table 1
Density and crystallinities for amorphous a-PS and s-PS and melt-crystallized s-PS samples

Material	Density (g/cm³) (± 0.0005)	X_C	τ_3 (ns)	τ_4 (ns)	I_3 (%)	I_4 (%)
Amorphous a-PS	1.0460	0	0.6 ± 0.3	2.06 ± 0.03	9 ± 2	30.4 ± 0.5
Amorphous s-PS	1.0490	0	0.9 ± 0.2	2.10 ± 0.03	8 ± 3	27.2 ± 0.5
α procedure						
1 min	1.0483	0.05 ± 0.04	0.8 ± 0.2	2.10 ± 0.04	7 ± 2	26.4 ± 0.3
5 min	1.0469	0.13 ± 0.04	0.7 ± 0.1	2.08 ± 0.04	9 ± 2	27.0 ± 0.4
15 min	1.0449	0.26 ± 0.04	0.6 ± 0.2	2.06 ± 0.03	13 ± 3	26.4 ± 0.3
30 min	1.0446	0.28 ± 0.04	0.8 ± 0.2	2.10 ± 0.04	8 ± 3	25.6 ± 0.4
45 min	1.0451	0.25 ± 0.04	0.6 ± 0.2	2.07 ± 0.03	11 ± 3	27.0 ± 0.4
60 min	1.0450	0.25 ± 0.04	0.6 ± 0.2	2.07 ± 0.03	12 ± 3	27.4 ± 0.5
90 min	1.0452	0.24 ± 0.04	0.7 ± 0.2	2.08 ± 0.02	10 ± 2	25.6 ± 0.3
180 min	1.0442	0.29 ± 0.04	0.8 ± 0.1	2.07 ± 0.04	5 ± 2	26.8 ± 0.2
β procedure						
15 min[a]	1.0501	0.05 ± 0.04	0.8 ± 0.2	2.08 ± 0.03	8 ± 2	28.2 ± 0.4
15 min[b]	1.0502	0.06 ± 0.04	0.5 ± 0.2	2.02 ± 0.04	15 ± 3	28.7 ± 0.3
30 min[a]	1.0535	0.24 ± 0.03	0.5 ± 0.1	2.03 ± 0.04	12 ± 2	26.1 ± 0.3
30 min[b]	1.0522	0.17 ± 0.03	0.8 ± 0.1	2.07 ± 0.04	7 ± 3	28.0 ± 0.4
60 min[a]	1.0549	0.31 ± 0.03	0.5 ± 0.2	2.01 ± 0.03	9 ± 2	27.1 ± 0.5
60 min[b]	1.0559	0.36 ± 0.03	0.6 ± 0.1	2.02 ± 0.01	7 ± 2	26.8 ± 0.4

[a] First run at making the samples.
[b] Second run at making the samples.

In analyzing the 5 million count spectra all three-component fits had variances greater than 1.3, whereas the four-component fits had variances less than 1.08. The lifetime and intensities derived from four-component fits to both the 1.5 and 5 million count spectra were comparable. Therefore, all data presented here are based on four-component fits of the 1.5 million count spectra.

Note that the ability to determine four components appears to be a result of using 4096 channels in the data acquisition, rather than the typical 1024 channels. This was confirmed by converting the 4096 channel spectra to 1024 channels (adding together the counts in 4 consecutive channels), and re-analyzing the resulting spectra with PATFIT. The three- and four-component fits of the 1024 channel spectra resulted in all variances being between 1.06 and 1.2, with neither fit being better than the other.

Table 1, lists the PALS parameters I_3 and τ_3, and I_4 and τ_4, measured at room temperature, for amorphous a-PS and s-PS as well as for semicrystalline s-PS specimens containing α and β crystal forms. Four PALS components have been reported to exist in several other amorphous and semicrystalline polymers [16,22,32]. It is well known that typical *ortho*-positronium lifetimes for amorphous polymers in the glass and rubbery states lie between 1.0 and 5 ns. The lifetimes of the fourth PALS component observed for amorphous a-PS and amorphous s-PS in this work, as evident in Table 1, are within this range, indicating that the fourth component is the result of *ortho*-positronium annihilation in the free-volume sites of the amorphous phase. The third PALS lifetime is much shorter than the fourth component, and has been attributed to various sources, including the effect of impurities on *ortho*-positronium annihilation [21,23], or to an annihilation mechanism other than via *ortho*-positronium formation. It is relevant here to point out that similar data were collected and analyzed for a specimen of poly(ethylene terephthalate) (PET) using the same apparatus, data acquisition and analysis procedure. Only three components could be extracted, even from a 5 million-count spectrum. Hence, the existence of an additional shorter lifetime component in a-PS and s-PS is certainly not an artifact from some quirk of data acquisition and analysis, but must be related to a difference in e^+ annihilation behavior related to the particular chemical structure of various polymers. It is important to note both three and four-component fits result in *ortho*-positronium lifetime and intensities with negligible differences. Only the smaller positron lifetime components, which are not relevant to our analysis, are affected by the choice of lifetime components.

Before discussing these PALS results further, we note that, on prolonged exposure to e^+ radiation, damage effects are known to accumulate in polymeric materials [33]. In many polymers, the effect is manifested by a decrease in the measured intensity of *ortho*-positronium annihilation with exposure time at temperatures below the glass transition [27–29]. The intensity changes are reversed on increasing
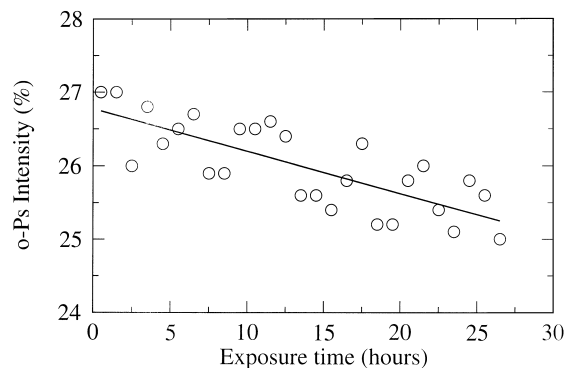

Fig. 4. Time dependence of *ortho*-positronium intensity for α-s-PS at 23 °C.

the temperature above T_g, suggesting that the effect is due to the accumulation of species which compete with e^+ for electrons in the glass, but which are rendered inactive by thermal motion in the melt. This phenomenon has been studied in a-PS [27] and our first effort in this work was to confirm that a similar problem exists in s-PS. Fig. 4 shows the change in intensity of the fourth lifetime component with increasing exposure time at room temperature. The radiation damage resulted in a decrease of about 8% over a period of one day for semicrystalline s-PS containing α form. From Fig. 4 it seems safe to assume that within a relatively short period of time, 1.5 h, the radiation effect is minimal and can be disregarded. For this reason, we rigorously adhered to a protocol such that all samples subjected to PALS analysis had the same radiation exposure time (1.5 h). Thus we feel secure that differences noted between s-PS and a-PS specimens are not a reflection of differences in radiation damage.

The intensities of the third lifetime components for amorphous a-PS and s-PS were similar within experimental error. The fourth lifetime component intensity, on the other hand, for amorphous a-PS is slightly larger, by 12%, than that for the amorphous s-PS. The origin of this small but significant difference is not clear. It may reflect that the effect of radiation damage is for some reason accelerated in a-PS versus s-PS. Since the densities of amorphous a-PS and s-PS are the same to within less than 1%, and likewise for the van der Waals volumes, the difference cannot arise from a difference in the total amount of free-volume. It could arise from a difference in the free volume distribution. Specifically, mesomorphic precursors to the crystal state may have small voids that are below the threshold of PALS detection. For example, in a PALS study of free volume in a thermotropic liquid crystal polymer [34], the *ortho*-positronium annihilation intensity strongly increases with temperature, which reflects the thermal expansion of small voids above the PALS detection threshold.

The third lifetime components determined for semicrystalline s-PS containing α and β crystalline structures are essentially indistinguishable from each other, and likewise for the fourth component lifetime. These lifetimes are also comparable to those observed for amorphous s-PS and a-PS.
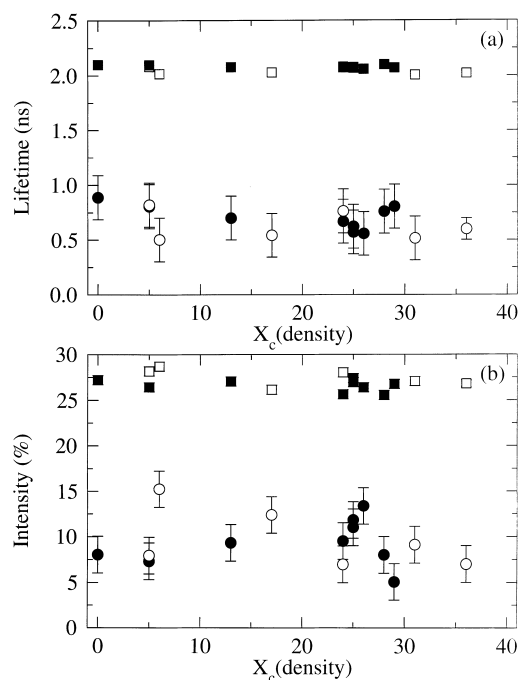
Fig. 5. Dependence of positron lifetime (a) and intensity (b) on crystallinity for syndiotactic-polystyrene of α (●—τ_3, I_3; ■—τ_4, I_4) and β (○—τ_3, I_3; □—τ_4, I_4) crystal forms.

Of particular interest is our observation in Table 1 that the intensities of the fourth lifetime components for amorphous and semicrystalline s-PS are all essentially the same, even for samples containing 43% crystallinity, i.e. lifetimes and intensities are independent of crystallinity, as shown pictorially in Fig. 5.

We now compare the PALS parameters obtained in this work with those derived previously by Dammert et al. [24] for an a-PS sample, and a semicrystalline s-PS sample containing the α crystal form. The longest living PALS components in this work (fourth component) for all PS samples had lifetimes in the range of 2.01 ± 0.03–2.10 ± 0.03 ns, in excellent agreement with the results of Dammert et al. who obtained lifetimes between 2.07 ± 0.02 and 2.11 ± 0.01 ns. However, the intensity of the fourth component in our work shows some disparities with the observations of Dammert et al. First, the intensities
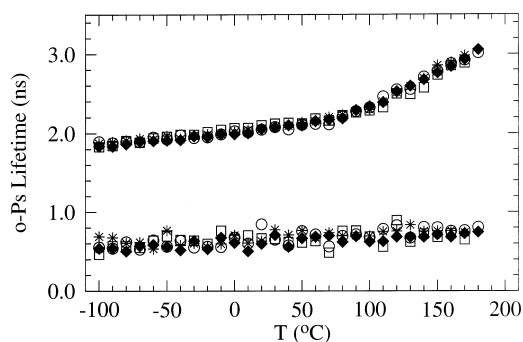

Fig. 6. Temperature dependence of *ortho*-positronium lifetime for amorphous s-PS (○), α-s-PS (□), β-s-PS (◆) and a-PS (∗).

measured in our studies for the s-PS samples containing the α form are slightly lower than that of the a-PS samples in this work, similar to the trend observed by Dammert et al., except that the difference is smaller ($\sim 12\%$) in our work versus (31%) in Dammert et al. However, more significantly, the intensity value determined in our work for amorphous s-PS is smaller than that for a-PS and numerically comparable to those values obtained for the semicrystalline s-PS specimens containing either α or β crystalline forms. Thus, our results indicate that, contrary to the conclusion of Dammert et al., *ortho*-positronium can indeed form in the α and β crystal phases of s-PS (Fig. 5).

To further delineate possible differences between semicrystalline s-PS, amorphous s-PS and amorphous a-PS, four samples were subjected to a temperature scan from -100 to $170\,°C$ was performed (viz. amorphous s-PS, amorphous a-PS, semicrystalline s-PS containing 25% α form and 31% β form). For all temperatures, the four-component fit was again slightly better than the three-component fit. As shown in Fig. 6, all four polymers exhibit essentially the same temperature dependence of τ_3 and τ_4. Typical for *ortho*-positronium annihilation in free volume of amorphous polymers, τ_4 exhibits an abrupt change in slope at T_g. Interestingly, τ_3 is essentially temperature independent through T_g, confirming that τ_3 is not a measure of the free-volume properties of the amorphous phase. Unfortunately, because of significant influence of radiation damage during the generation of these data, which involved exposure of the sample over a period of 2.5 days, it is not possible to interpret the corresponding intensities, I_3 and I_4.

Our results clearly demonstrate that the *ortho*-positronium lifetimes and intensities in s-PS containing either α or β crystalline forms are very similar to that of amorphous s-PS, and indeed independent of the degree of crystallinity. This observation is new, and has never been reported. The most obvious explanation of this result is that *ortho*-positronium can form and annihilate in the low-density α and β crystalline phase of s-PS, as well as in the amorphous phase. In such a case, the intensity would not be affected by the crystallinity; however, the lifetime would have to be remarkably similar for both the α and β crystalline forms, and for the amorphous phase. It is not immediately obvious that channels could exist in the β crystalline form; however, given that the density of this crystalline form is only 1% denser than the amorphous phase, it seems likely that it has a relatively large amount of open space. Furthermore, it is well accepted that the β crystals have T4 conformational order, therefore, it is reasonable that large contiguous voids can be formed along the trans–trans orientation, through which the relatively small *ortho*-positronium probe would easily traverse. To clarify the possibility of *ortho*-positronium annihilation in the putative nanochannels of the α and β crystals structure, we carried out a theoretical analysis of the expected lifetime of *ortho*-positronium trapped in cylindrical cavities as a function of the diameter and length.

3.3. ortho-Positronium annihilation in cylindrical cavity

It is typically assumed that *ortho*-positronium annihilates in spherical free-volume holes of the amorphous phase of polymers with a lifetime strongly dependent on the size of the hole. An equation relating the free-volume hole size to *ortho*-positronium lifetime has been derived using quantum mechanical calculations, which assume that *ortho*-positronium is trapped in a spherical void having an infinite potential energy at the boundary. Without taking into account an *ortho*-positronium interaction with the electrons of the structure, the lifetime will be 142 ns (vacuum lifetime), independent of void size. To account for the interaction of *ortho*-positronium with the polymer matrix, a thin electron layer is considered to exist at the boundary of the void [35,36]. By comparing PALS annihilation data to molecular solids of known pore sizes [35,37], the electron layer thickness has been determined to be 0.1656 nm. The resulting semiempirical equation relating the free-volume hole radius, R, to the measured *ortho*-positronium lifetime, τ, and electron layer thickness d, is given by

$$\tau = \frac{1}{2}\left[1 - \frac{R}{R+d} + \frac{1}{2\pi}\sin\left(\frac{2\pi R}{R+d}\right)\right]^{-1} \quad \text{(ns)} \quad (1)$$

Using the same basic quantum mechanical calculation (i.e. the same Schrödinger equation), but converting from spherical to cylindrical coordinates, the lifetime equation for *ortho*-positronium in a cylindrical cavity can be derived. For a cylindrical cavity of radius R, and length L, and electron layer thickness, d, the *ortho*-positronium lifetime is

$$\tau = \tfrac{1}{2}(1 - P_1 P_2)^{-1} \quad \text{(ns)} \quad (2)$$

where

$$P_1 = \frac{L}{L+d} + \frac{1}{\pi}\sin\left(\frac{\pi L}{L+d}\right) \quad (3)$$

$$P_2 = \frac{\displaystyle\int_0^{a_1(R/(R+d))} x J_0^2(x)\,\mathrm{d}x}{\displaystyle\int_0^{a_1} x J_0^2(x)\,\mathrm{d}x} \quad (4)$$

with $J_0(x)$ the Bessel function of the first kind of order zero, and a_1 the first zero of $J_0(x)$ (2.4048). The same electron layer thickness, $d = 0.1656$ nm, as that in the semiempirical equation for *ortho*-positronium trapped in a spherical cavity was assumed.

The dependence of lifetime, τ, on cylinder radius, numerically calculated from Eq. (2), is shown in Fig. 7, for various cylinder lengths, including an infinitely long cylindrical cavity and a cylindrical cavity of equal length and diameter. The lifetime dependence for *ortho*-positronium trapped in spherical cavities calculated from Eq. (1) is also shown in Fig. 7 as a function of cavity radius, R. It is anticipated that the lifetime for a spherical cavity as a function of R calculated from Eq. (1) must be very similar to that calculated from Eq. (2) for a cylindrical cavity of radius
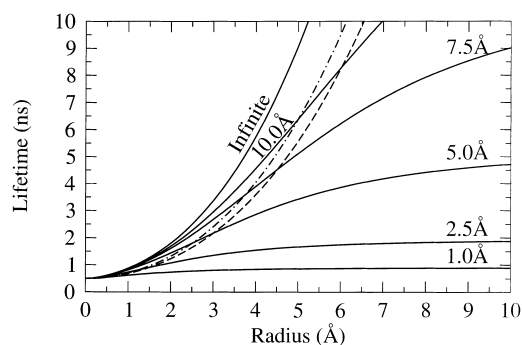

Fig. 7. *ortho*-Positronium lifetime dependence on radius for cylindrical holes of 1, 1.5, 5, 7.5, 10 Å and infinite length (Eq. (2)) (−), a cylindrical box of $L = 2R$ (Eq. (2)) (−·−) and a spherical hole (Eq. (1)) (− − −).

R, and length $2R$. Indeed, similar lifetimes are predicted for the same R as evident in Fig. 7. Also evident in Fig. 7, the lifetime of *ortho*-positronium trapped in cylindrical cavities is very sensitive to small cavity lengths, i.e. smaller than 10 Å. Using the lamellar thickness of 100 Å for semicrystalline s-PS [5] as an estimate of channel length, we conclude that the lifetime must correspond rather closely to the solution of Eq. (2) for an infinitely long cylindrical cavity.

Thus we can deduce that *ortho*-positronium, trapped in infinitely long cylinders of 1.5–2.5 Å radius, which corresponds to the channel widths in the α crystal structures proposed by De Rosa and Gries (Fig. 1), is expected to have a lifetime in the range of 1.3–2.5 ns. Using similar arguments, a much shorter lifetime is expected in the case of the β form, due to the smaller voids between the chains. Interestingly, the range of theoretically predicted lifetimes for the α crystal form brackets the experimental lifetime, 2.1 ns, determined at room temperature for s-PS. Therefore, the lifetimes corresponding to positron annihilation in the spherical cavities of the amorphous phase and cylindrical cavities of the α crystalline phase may be very similar at room temperature, making it very difficult to experimentally distinguish these two very different annihilation processes. In turn, for lifetimes shorter than 1.3 ns, as theoretically expected for β crystalline form, the same overlap problem can be foreseen with the third PALS lifetime parameter of about 0.7 ns.

At higher temperatures, the amorphous lifetime may increase sufficiently to extract the lifetime associated with the α crystalline form, which is expected to be less temperature dependent. The PALS spectra of s-PS containing the α and β crystalline forms at different temperatures (Fig. 6) were, therefore, analyzed for five PALS components. A fifth lifetime was not extractable at any temperature, and indeed the fits to four components became statistically better at the highest temperatures, with $\tau_4 \geq 2.4$ ns.

Therefore, we need to consider the possibility that *ortho*-positronium may form in, but not annihilate in the α and β crystal phases. Thus, we assume that once

formed, *ortho*-positronium can diffuse out of the channel and annihilate in the amorphous phase. A simple calculation of the thermal velocity of an e^+-e^- pair can provide a reasonable estimate of how long it takes for positronium to traverse the length of a nanochannel (100 Å). The mean velocity, *u*, is of the order of $(kT/m)^{1/2}$, where $m = 2m_e$. Thus, the mean velocity for positronium at room temperature is of the order of 10^4 m/s (100 Å/ps), which allows the *ortho*-positronium to travel the entire length of a 100 Å channel in 1 ps. Therefore, we conclude that *ortho*-positronium has a very high probability, once formed, to leave the nanochannel and hence annihilate in the amorphous phase with a lifetime characteristic of this phase. This explains why the intensity of *ortho*-positronium annihilation does not depend on the crystallinity, since it can form both the amorphous and crystalline phases, yet the lifetime is characteristic of the amorphous phase only. Given that the proposed nanochannels are constructed from the phenyl rings of the polystyrene chains, they are surrounded by an electron layer, which will act to confine positronium toward the center, increasing the probability of it traveling the length in a time comparable to 1 ps. This process is similar to the way in which positronium is believed to be very quickly localized in free-volume in the amorphous phase by repulsion between the electron of the positronium and the electrons of the matrix.

We must also consider that *ortho*-positronium once formed, appears to diffuse through the β phase of s-PS as easily as it does through the less dense α phase. Here, it is pertinent to note that the size of the *ortho*-positronium probe is about 1.1 Å, which is much smaller than the voids between chains in both α and β crystalline s-PS forms. The mechanism by which *ortho*-positronium forms in, and rapidly diffuses out of the channels in the α crystalline phase of s-PS is reminiscent of that proposed to explain the unusual gas transport behavior observed in semicrystalline s-PS containing the α crystalline form [9,10]. As noted earlier, gas permeation measurements indicate that O_2 and CO_2 easily pass through the α crystalline phase of s-PS. Analysis of these data indicates that the α phase shows very low oxygen and carbon dioxide solubility in comparison to the amorphous phase. Thus, the porous α structure serves the role of a transmitting medium in semicrystalline s-PS, making a negligible contribution to the overall gas sorption, but significantly accelerating the diffusion process by enabling gas molecules to pass through the long nanochannels in the crystal structure. It was further found that the β form is less permeable than the α form for oxygen and carbon dioxide, which reflects the relatively large gas molecule sizes of about 3.4–3.9 Å [38]. The smaller *ortho*-positronium species is apparently not sensitive to the different crystal packing densities of the α and β phases.

4. Conclusions

PALS measurements were performed on amorphous a-PS and amorphous s-PS along with a series of s-PS samples crystallized from the melt state. The semicrystalline s-PS samples contained either pure α or β forms with various crystallinities. The effect of crystallinity, crystalline structure, tacticity, and temperature on PALS parameters was investigated. In analyzing the PALS spectra, it was found that four distinct lifetime components gave the best fit for all samples. The longest lifetime component ($\tau_4 = 2-3$ ns) exhibits behavior typical of amorphous polymers, while the second largest lifetime ($\tau_3 \sim 0.8$ ns) is found to be constant, independent of temperature, crystallinity and tacticity. The origin of the third component is not currently understood.

For all semicrystalline and amorphous s-PS samples, the PALS spectra were found to be essentially indistinguishable, with remarkably similar *ortho*-positronium lifetimes and intensities. The *ortho*-positronium lifetime for amorphous a-PS was also similar to that of the s-PS samples, however, the intensity of the fourth component was slightly larger. The origin of this small but significant difference is not exactly clear, however, it may be due to a difference in the distribution of free-volume between the two polymers. It is surprising that no difference in PALS spectra were found for semicrystalline s-PS containing either pure α or β crystalline structures.

The similarity of *ortho*-positronium intensities for semicrystalline s-PS containing α and β forms of various crystallinities suggests that *ortho*-positronium is not only formed in the amorphous phase, but also forms in nanochannels of the α and β structures. Quantum mechanical calculations were performed to analyze the *ortho*-positronium lifetime trapped in a cylindrical cavity of different dimensions. The calculation predicts that, in channels with an aperture of 3–5 Å and a length of about 100 Å, characteristic of the α crystal structure, the lifetime, τ_4, is comparable to that measured at room temperature in the amorphous phase, but should be sufficiently different to distinguish at high temperatures, where the amorphous lifetime component is large. However, at all temperatures only four lifetime components were found. This leads us to conclude that *ortho*-positronium, once formed in the crystalline structure, diffuses to the amorphous phase where it subsequently annihilates.

References

[1] Guerra G, Vitagliano VM, De Rosa C, Petraccone V, Corradini P. Macromolecules 1990;23:539.
[2] Chatani Y, Fujii Y, Shimane Y, Ijitsu T. Polym Prepr Jpn (Engl Ed) 1988;37:E428.
[3] Sun Z, Morgan RJ, Lewis DN. Polymer 1992;33:661.
[4] Van Krevelen DW. Properties of polymers, 3rd ed. New York: Elsevier; 1990.
[5] Greis O, Xu Y, Asano T. Polymer 1989;30:590.
[6] De Rosa C, Guerra G, Petraccone V, Corradini P. Polym J 1991;23: 1435.
[7] De Rosa C, Rapacciuolo M, Petraccone V, Corradini P. Polymer 1992;33:1423.
[8] Zoller P. J Appl Polym Sci 1977;21:3129.
[9] Hodge K, Prodpran T, Shenogina NB, Nazarenko SJ. J Polym Sci, Part B: Polym Phys 2001;15:2519.
[10] Prodpran T, Shenogin S, Nazarenko S. Polymer 2002;43:2295.
[11] Stevens JR, Methods of experimental physics, vol. 16A. New York: Academic Press; 1980. p. 371.
[12] Jean YC. Microchem J 1992;42:72.
[13] Pethrick RA. Prog Polym Sci 1997;22:1.
[14] Srithawatpong R, Peng ZL, Olson BG, Jamieson AM, Simha R, McGervey JD, Maier TR, Halasa AF, Ishida H. J Polym Sci, Part B: Polym Phys 1999;37:2754.
[15] Yu Z, Yahsi U, McGervey JD, Jamieson AM, Simha R. J Polym Sci, Part B 1994;32:2637.
[16] Dlubek G, Stejny J, Lupke T, Bamford D, Petters K, Hubner C, Alam MA, Hill MJ. J Polym Sci, Part B: Polym Phys 2002;40:65.
[17] Nakanishi H, Jean YC, Smith EG, Sandreczki TC. J Polym Sci, Part B: Polym Phys 1989;27:1419.
[18] Welander M, Maurer FHJ. Mater Sci Forum 1992;105:1811.
[19] Dlubek G, Stolp M, Nagel C, Fretwell HM, Alam MA, Radusch HJ. J Phys: Condens Matter 1998;10:10443.
[20] Mohamed HFM, Ito Y, Imai M. J Chem Phys 1996;105:4841.
[21] Kindl P, Puff W, Sormann H. Phys Status Solidi, Part A 1980;58:489.
[22] Madani MM, Macqeen RC, Granata RD. J Polym Sci, Part B: Polym Phys 1996;34:2770.
[23] Reiter G, Kindl P. Phys Status Solidi, Part A 1990;118:161–8.
[24] Dammert RM, Maunu SL, Maurer FHJ, Neelov IM, Niemela S, Sundholm F, Wastlund C. Macromolecules 1999;32:1930.
[25] Kluin JE, Vleeshowers S, McGervey JD, Jamieson AM, Simha R, Sommer K. Macromolecules 1993;26:1853–61.
[26] Kirkegaard P, Eldrup M, Mogensen OE, Pedersen NJ. Comp Phys Commun 1981;23:307.
[27] Peng ZL, Olson BG, McGervey JD, Jamieson AM. Polymer 1999;40: 3033.
[28] Welander M, Maurer FHJ. Mater Sci Forum 1992;105:1815.
[29] Li XS, Boyce MC. J Polym Sci, Part B 1993;31:869.
[30] Cartier L, Okihara T, Lotz B. Macromolecules 1998;31:3303.
[31] Pasztor Jr AJ, Landes BG, Karjala P. J Thermochim Acta 1991;177: 187.
[32] McGervey JD, Olson BG, Peng ZL, Jamieson AM, Simha R. Mater Sci Forum 1997;255:763.
[33] Maurer FHJ, Welander M. J Adhes Sci Technol 1991;5:425.
[34] McCullagh CM, Yu Z, Jamieson AM, Blackwell J, McGervey JD. Macromolecules 1995;28:6100.
[35] Eldrup M, Lightbody D, Sherwood JN. Chem Phys 1981;63:475.
[36] Tao SJ. J Chem Phys 1972;56:5499.
[37] Nakanishi H, Jean YC. Positron and positronium chemistry. Amsterdam: Elsevier; 1988. p. 167.
[38] Hedenqvist M, Gedde UW. Prog Polym Sci 1996;21:299.